PHYSICAL REVIEW E

STATISTICAL PHYSICS, PLASMAS, FLUIDS, AND RELATED INTERDISCIPLINARY TOPICS

THIRD SERIES, VOLUME 55, NUMBER 4 **APRIL 1997**

RAPID COMMUNICATIONS

The Rapid Communications section is intended for the accelerated publication of important new results. Since manuscripts submitted to this section are given priority treatment both in the editorial office and in production, authors should explain in their submittal letter why the work justifies this special handling. A Rapid Communication should be no longer than 4 printed pages and must be accompanied by an abstract. Page proofs are sent to authors.

Experimental observation of a chaotic attractor with a reverse horseshoe topological structure

G. Boulant, S. Bielawski, D. Derozier, and M. Lefranc

Laboratoire de Spectroscopie Hertzienne, URA CNRS 249, Centre d'Etudes et de Recherches Lasers et Applications, Université de Lille I, F-59655 Villeneuve d'Ascq Cedex, France

(Received 31 December 1996)

We have characterized the topological organization of chaotic regimes of a modulated Nd:YAG (yttrium aluminum garnet) laser using template analysis. This investigation revealed a topological structure not previously observed in an experimental system nor in numerical simulations of models of this laser to our knowledge. This structure corresponds to the so-called reverse horseshoe theoretically described by Gilmore and McCallum [Phys. Rev. E **51**, 935 (1995)]. [S1063-651X(97)50104-8]

PACS number(s): 05.45.+b, 42.65.Sf, 42.55.Rz

The experimental study of a system displaying chaotic behavior requires characterization methods which can extract in a robust way the invariant properties of a chaotic regime from apparently erratic signals. This is usually done by reconstructing a strange attractor, an invariant set of the phase space which the asymptotic dynamics is confined to, and analyzing this highly complex geometrical object (see, e.g., [1]). Traditionally, quantitative measures of chaos have focused on global statistical properties of the attractor, such as fractal dimensions or Lyapunov exponents [1].

However, attractors are not the only invariant sets of chaotic dynamics. In recent years, there has been an increased interest in using unstable periodic orbits (UPO) to characterize chaotic attractors. Indeed, a typical chaotic attractor has embedded in it a dense set of UPO, and one may reasonably hope to use these to approximate the attractor in a hierarchical way: low-period orbits model the overall structure of the attractor, while finer details can be resolved using higher-period ones (see, e.g., [2]). Of particular importance is the fact that UPO can be extracted from experimental time series.

In the phase space of the system, unstable periodic orbits are represented by closed curves. While these are relatively simple objects, they are intertwined in a very complex way due to the chaotic dynamics. For three-dimensional systems with at most one positive Lyapunov exponent, the template analysis proposed by Mindlin *et al.* [3,4] allows one to unfold this complexity by analyzing UPO using concepts from knot theory [5,6]. For example, a pair of periodic orbits can be characterized by their linking number, which measures how many times one orbit winds around the other. The relevance of knot invariants to chaotic dynamics owes much to the fact that determinism precludes that different trajectories intersect. As a consequence, linking numbers and other topological invariants remain constant as a control parameter is varied. Additionally, their invariance with respect to small deformations makes their experimental determination quite insensitive to noise, provided periodic orbits are well separated.

Moreover, a systematic study of the topological organization of the UPO embedded in a chaotic attractor is allowed by the existence of a two-dimensional branched manifold, the *template* (or ''knot-holder'') [7,8], such that all the periodic orbits can be laid on it without modifying any of their topological invariants. The template, whose structure can be concisely described by small integer matrices [3], thus describes the global topological organization of the chaotic attractor. Experimentally, measuring the invariants of a few periodic orbits suffices to determine the associated template, the remaining orbits being used to check the validity of the results [4].

As advocated by their authors [3,4,9], one distinct advantage of this approach is its ability to give a clear-cut

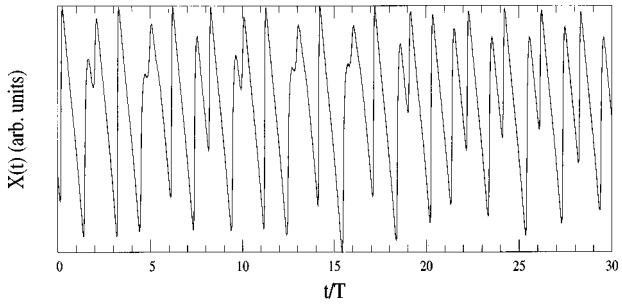

FIG. 1. Time series of $X(t)=\log(I+I_0)$ where I is the laser output intensity and I_0 is a small constant which can be adjusted in the logarithmic amplifier used for signal processing. T is the modulation period.

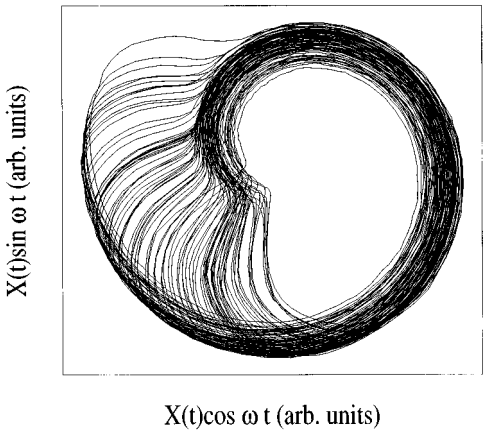

FIG. 2. Phase portrait of the attractor in the plane $[X(t)\cos\phi, X(t)\sin\phi]$, where $\phi=\omega t$ is the modulation phase.

answer as to whether a theoretical model is incompatible with given experimental data. If the analysis of experimental time series and of time series generated from numerical simulations of a model, embedded in the same phase space, yields different templates, then this model, at least for the values of the parameters used in the simulations, has to be rejected.

However, except for a catalytic reaction whose template has unfortunately not been exactly determined [10], most experimental investigations so far, in optics [9,11–13], in chemistry [4,14] or mechanics [15], have revealed the same topological structure, namely the one described by the so-called Smale's horseshoe with zero global torsion. Horseshoe templates with global torsions have been observed in an optical fiber laser [16]. One may then wonder whether the horseshoe class is so ubiquitous as to make template analysis helpless for testing the relevance of a model.

In this Communication we show that this is not the case, by reporting the observation of regimes of a Nd:YAG (yttrium aluminum garnet) laser with pump modulation that are associated with a different type of template. The corresponding topological organization has been theoretically predicted to be observable in nonlinear driven oscillators by Gilmore and McCallum [17] (they termed it ''reverse horseshoe''), but to our knowledge has not yet been encountered in other experiments, nor in numerical studies of models of this type of laser. While this template has a two-branch structure as is the case of the above-mentioned templates, the difference is readily shown by analyzing the lowest-period orbits: the period-$2T$ orbit (T is the modulation period) is unknotted, but the knot type of the period-$3T$ orbits is that of a trefoil knot, the simplest knot beyond a trivial loop. In contrast to this, the period-$2T$ and $3T$ orbits of experimental chaotic attractors characterized by topological analysis were either all unknotted [4,9,11–15] or all knotted [16].

The experimental system consists of a Fabry-Perot laser cavity, end-pumped by a cw laser diode operating at 812 nm. The Nd:YAG rod is 10 mm long, 7 mm in diameter, and contains a nominal Nd^{3+} concentration of 1.1%. One of the two plane ends is highly reflective at the laser wavelength (1064 nm), and the other is antireflection coated. The output coupler is concave, with a radius of curvature of 40 mm, and has a reflectivity of 97%. A Fabry-Perot etalon and a Brewster plate are inserted inside the cavity to select single-mode oscillation on a linear polarization. In these conditions, the pump parameter A (the ratio of pump power to its value at threshold) can range up to 3. In our experiment, the pump power is sinusoidally modulated, $A=A_0(1+m\cos\omega t)$, and the laser undergoes a classical period-doubling cascade leading to chaos when the frequency modulation is of the order of the relaxation frequency ω_r of the laser, which is about 100 kHz here. In this paper, the topological organization of a chaotic regime for parameters $A_0=1.2$, $m=0.5$, and $\omega=54$ kHz, is analyzed. It should be noted that as the resonance frequency markedly decreases when the modulation amplitude is increased, these parameters in fact belong to the resonance tongue originating at $\omega=\omega_r$. The laser output intensity was monitored with a $In_xGa_{1-x}As$ detector, and processed using a logarithmic amplifier in order to obtain a signal suitable for topological analysis (see, e.g., [12]). The present analysis has been carried out on a time series corresponding to 5×10^3 periods of modulation, recorded at a rate of 100 samples per modulation period. A typical signal is shown in Fig. 1.

Let us now briefly describe the procedure of the analysis. First, unstable periodic orbits are extracted from the time series using close return techniques similar to those described in Refs. [4,9,12,13]: a time series segment $\{X(t);t_0<t<t_0+nT\}$ is considered to shadow an unstable period-nT orbit if $|X(t)-X(t+nT)|<\epsilon$ for each $X(t)$ belonging to that segment, where ϵ is in the order of a few percent. Doing so, we detected eight orbits, with periods up to $9T$.

These periodic segments then have to be embedded in a phase space, so that the topological invariants of the corresponding trajectories can be computed. As in previous investigations [12,13], we embedded the time series in a phase space with cylindrical coordinates $[X(t),\dot{X}(t),\phi(t)]$, where $\phi(t)=\omega t \bmod 2\pi$ is the modulation phase. A plane phase portrait of the embedded attractor is displayed in Fig. 2, and a first return map in a section plane of constant phase is plotted in Fig. 3. We recall that the analysis does not require the actual computation of the time derivative of $X(t)$. Rather, given a time series segment corresponding to a period-nT orbit, a simple plot of $X(\phi(t))$ versus $\phi(t)$ displays the orbit as a braid on n strands (see, e.g., [12,13]), as can be seen in Fig. 4. Listing the crossings which occur as ϕ is increased from 0 to 2π gives an algebraic description of the braid, the braid word [6], from which the various topological invariants

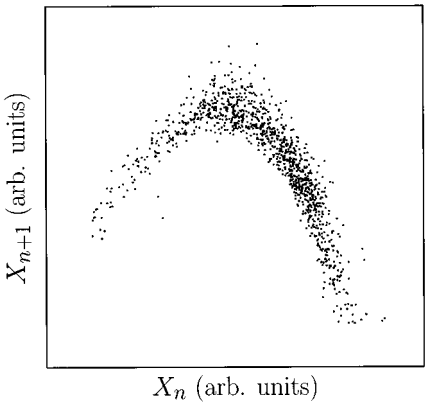

FIG. 3. First return diagram X_{n+1} vs X_n, where $X_n = X(t_0 + nT)$ is a stroboscopic sampling of the signal, and T is the modulation period. This map corresponds to a section plane of constant modulation phase. It can be seen to be highly similar to those observed in systems whose topological organization is described by the standard Smale's horseshoe template.

can be computed. One distinct feature of the embedding we have used is that periodic orbits are naturally presented as positive braids, i.e., all their crossings have the same sign, which can be chosen to be positive. This implies that the entries of the template matrix, which are directly related to the torsions and linking numbers of period-T orbits [3,4], are positive. This property will be of particular importance in the foregoing discussion.

Table I displays the (self-) linking numbers of the lowest-period orbits detected in our experiment. Given this information about the relative placement of the UPO, we may now seek a template that holds a set of periodic orbits with identical periods and topological invariants. As usual, the template branches are labeled ''0,'' ''1,'' . . . , starting from the leftmost branch. We find that two two-branch templates are compatible with the experimental data. They correspond to two equivalent representations of the same topological structure, and can be distinguished according to whether the orbit corresponding to the experimental period-T orbit is located on the ''0'' or the ''1'' branch of the template. For definiteness, and to ease comparison with other works, let this orbit be held by the ''1'' branch. The template matrix of the corresponding solution reads

$$\mathcal{T} = \begin{pmatrix} 2 & 2 \\ 2 & 1 \end{pmatrix}, \tag{1a}$$

with the insertion matrix being

$$\mathcal{I} = (0 \quad -1). \tag{1b}$$

This result is to be contrasted with the standard horseshoe template, whose template and insertion matrices are given by

$$\mathcal{T}_\theta^{\mathrm{HS}} = \begin{pmatrix} 2\theta & 2\theta \\ 2\theta & 1+2\theta \end{pmatrix} = \begin{pmatrix} 0 & 0 \\ 0 & 1 \end{pmatrix} + \theta \begin{pmatrix} 2 & 2 \\ 2 & 2 \end{pmatrix} \tag{2a}$$

$$\mathcal{I}_\theta^{\mathrm{HS}} = (0 \quad 1), \tag{2b}$$

where the integer θ stands for the global torsion.

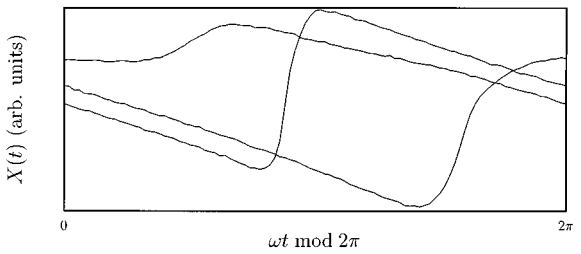

FIG. 4. A time series segment shadowing one of the period-$3T$ orbits is plotted as a function of $\phi(t) = \omega t \bmod 2\pi$. This presents this orbit as a braid on three strands. The number of crossings in this plot gives the self-linking number of the orbit which here is 4. This value is to be contrasted with that obtained for standard horseshoe templates, i.e., $2+6\theta$, where the integer θ is the global torsion.

It should be recalled that, depending on the sign conventions, the same system can be described by two templates differing only by their handedness. However, when using, as here, an embedding which forbids negative topological invariants, only one of them may be a solution. To compare our result to those of previous investigations, we thus choose in each case the sign convention leading to positive invariants. With this point in mind, the $\theta = 0$ case corresponds to the experiments reported in Refs. [4,9,11–15], while horseshoe templates with $\theta = 1$, 2, or 3 have been observed in an optical fiber laser [16].

Rewriting Eq. (1a) as

$$\mathcal{T} = \begin{pmatrix} 0 & 0 \\ 0 & -1 \end{pmatrix} + \begin{pmatrix} 2 & 2 \\ 2 & 2 \end{pmatrix}, \tag{3}$$

it is easily seen that the template we have observed is in fact the mirror image of the standard horseshoe template with zero global torsion [as described by Eqs. (2)], plus a global torsion of one turn. From the discussion above, it should be clear that this discrepancy with previous reports does not stem from an unfortunate choice of sign convention nor of phase-space orientation. Moreover, we do not think that the phenomenon recently described by Mindlin and Solari— under certain conditions the topology of an attractor may dramatically depend on the chosen embedding [18]—can ex-

TABLE I. Self-linking numbers and linking numbers of the lowest-period orbits detected in the experimental time series. The entries left blank correspond to invariants whose value could not be ascertained, because different estimates were obtained when using two different time series segments corresponding to the same orbit.

	$1T$	$2T$	$3T_a$	$3T_b$	$4T$	$5T$	$7T$	$9T$
$1T$	0							
$2T$	1	1						
$3T_a$	2	4	4					
$3T_b$	2	4	6	4				
$4T$	2	5	8		7			
$5T$	3	6	10	10		12		
$7T$		8	14	14			24	
$9T$	5		18					

plain our observations, since the attractors we studied are not split into several disjoint pieces. We can therefore conclude that our results are the signature of a different type of topological organization, and are not due to artifacts of the analysis.

What makes this result highly interesting is that previous template analyses of a modulated CO_2 laser [12,13], using the same embedding as here, found a horseshoe template with zero global torsion. Indeed, the Nd:YAG laser and the CO_2 laser are generally both considered to be class-B lasers, i.e., lasers where the polarization of the gain medium evolves much faster than the inversion population or the radiation intensity [19–21]. As a result, the single-mode behaviors of these two lasers can in principle be modeled by the very same set of equations, the so-called ''two-level rate equations'' [20,21], and correspond to parameters of the same order of magnitude. Furthermore, numerical studies of this model with parameters corresponding to the CO_2 experiments seemed to indicate that the topological organization of its chaotic regimes was globally described by the horseshoe template with zero global torsion [22], until a three-branch spiral template was discovered very recently for slightly different values of the control parameters [23]. As for the reverse horseshoe template that corresponds to our experiment, it remains to be observed in numerical simulations of the modulated class-B laser model.

To summarize, we are in a situation where (i) standard and reverse horseshoes have been observed in laser experiments, and (ii) standard horseshoes and a spiral three-branch template have been identified in numerical studies of these lasers. In view of the complex structure of the bifurcation diagram of nonlinear driven oscillators described by Gilmore and McCallum [17], this gives us some confidence that a systematic exploration of the parameter space of these systems using template analysis may provide an accurate test of the validity of the class-B laser model.

In conclusion, we performed a template analysis of chaotic regimes from a Nd:YAG laser. This characterization showed a topological organization of the reverse horseshoe type, which to our knowledge has not yet been observed experimentally. Topological analysis thus allowed us to unveil clear-cut differences from previous laser experiments which would likely have remained otherwise unnoticed, given the high similarity of the signals corresponding to standard and reverse horseshoes.

We believe that the present work certainly motivates further experiments and numerical investigations of the model describing both these lasers, and illustrates the relevance of template analysis in the study of the dynamical properties of low-dimensional chaotic systems.

The Laboratoire de Spectroscopie Hertzienne is Unité de Recherche Associée au CNRS. The Centre d'Études et Recherches Lasers et Applications is supported by the Ministère chargé de la Recherche, the Région Nord-Pas de Calais, and the Fonds de Développement Economique des Régions.

[1] E. Ott, *Chaos in Dynamical Systems* (Cambridge University Press, Cambridge, 1993).
[2] D. Auerbach *et al.*, Phys. Rev. Lett. **58**, 2387 (1987).
[3] G. B. Mindlin *et al.*, Phys. Rev. Lett. **64**, 2350 (1990).
[4] G. B. Mindlin *et al.*, J. Nonlinear Sci. **1**, 147 (1991).
[5] N. B. Tufillaro, T. A. Abbott, and J. P. Reilly, *An Experimental Approach to Nonlinear Dynamics and Chaos* (Addison-Wesley, Reading, MA, 1992).
[6] L. H. Kaufmann, *Knots and Physics* (World Scientific, Singapore, 1991).
[7] J. S. Birman and R. F. Williams, Topology **22**, 47 (1983).
[8] P. J. Holmes, in *New Directions in Dynamical Systems*, edited by T. Bedford and J. Swift (Cambridge University Press, Cambridge, 1988), pp. 150–191.
[9] F. Papoff *et al.*, Phys. Rev. Lett. **68**, 1128 (1992).
[10] S. O. Firle, M. A. Natiello, and M. Eiswirth, Phys. Rev. E **53**, 1257 (1995).
[11] N. B. Tufillaro *et al.*, Phys. Rev. A **44**, 4786 (1991).
[12] M. Lefranc and P. Glorieux, Int. J. Bifurcation Chaos Appl. Sci. Eng. **3**, 643 (1993).
[13] M. Lefranc *et al.*, Phys. Rev. Lett. **73**, 1364 (1994).
[14] C. Letellier, L. L. Sceller, and J. L. Hudson, J. Phys. C **99**, 7016 (1995).
[15] N. B. Tufillaro *et al.*, Phys. Rev. E **51**, 164 (1995).
[16] G. Boulant, M. Lefranc, S. Bielawski, and D. Derozier, Phys. Rev. E (to be published).
[17] R. Gilmore and J. W. L. McCallum, Phys. Rev. E **51**, 935 (1995).
[18] G. B. Mindlin and H. G. Solari, Phys. Rev. E **52**, 1497 (1995).
[19] F. T. Arecchi, in *Instabilities and Chaos in Quantum Optics*, edited by F. T. Arecchi and R. G. Harrison (Springer, Berlin, 1987), p. 9.
[20] L. M. Narducci and N. B. Abraham, *Laser Physics and Laser Instabilities* (World Scientific, Singapore, 1988).
[21] Y. I. Khanin, *Principles of Laser Dynamics* (Elsevier, Amsterdam, 1995).
[22] H. G. Solari and R. Gilmore, Phys. Rev. A **37**, 3096 (1988).
[23] G. Boulant, M. Lefranc, S. Bielawski, and D. Derozier, Int. J. Bifurcation Chaos Appl. Sci. Eng. (to be published).